

CHAPTER V

POTENTIAL BIODEGRADABLE MULCH FILM FROM POLY(LACTIC ACID)/SILANE-MODIFIED THERMOPLASTIC STARCH BLEND

5.1 Abstract

Poly(lactic acid) (PLA) blended with silane-modified thermoplastic starch (mTPS) film is proposed for the first time to use as fully biodegradable mulch film. Replacing TPS by mTPS, the remarkable miscibility enhancement with well mTPS dispersion in PLA matrix and the reduction of surface roughness are achieved although the mTPS content in the blend is as high as 50 %wt, as evidenced by SEM and AFM images. The miscible PLA/mTPS film allows not only the promoted PLA chains mobility (decreased T_g to 46 °C) and PLA chain regularization (increased X_c to ~50%) but also the significantly improved flexibility (ϵ 52%) as compared to PLA/TPS film (T_g 50 °C, X_c ~40%, and ϵ 25%). Additionally, the restrained oxygen permeability (from 50 to 20 cm³ mm/m² day atm) has been successfully obtained by the highly developed X_c combined with PLA/mTPS homogeneity. In contrast, an increase of oxygen permeability (90 cm³ mm/m² day atm) was found due to the PLA/TPS immiscibility. Moreover, the PLA/mTPS film performs higher tolerance to simulated weather with preserving film-form than that of PLA/TPS film, as investigated by QUV accelerated weathering.

Keywords: poly(lactic acid), thermoplastic starch, miscibility, silane modification, mulch film

5.2 Introduction

Recently, the interest of polymer films in agriculture is significantly increased, especially for mulching. The mulch film plays an important role on crop production such as inhibiting weed growth, maintaining soil moisture, and preserving nutrients in soil.^{1,2} Nonetheless, it generates the environmental issue of plastic waste because the general mulch films used are based on conventional plastics (*i.e.* low

density polyethylene (LDPE)³⁻⁵ and ethylene butyl acrylate (EBA)/ethyl vinyl acetate (EVA)⁶. They are always left on the field after harvesting or sometimes burnt uncontrollably, resulting in release of harmful substances, contaminating in soil. Moreover, the recycling of these mulch films is unattractive due to labor-intensive cost for removal, including time-consuming for collection.⁷ Therefore, the biodegradable mulch film becomes an effective solution since it is disposable directly into the soil. Up to the present, there are a few of commercial biodegradable mulch films such as poly(butylene adipate-*co*-terephthalate ((PBAT) or Ecoflex[®])⁸⁻¹⁰ and Mater-Bi[®] (a starch-based biodegradable polymer)¹¹, but they are not cost competitive with conventional polymers.

One of the most potential biodegradable plastics with reliable industrial-scale production is poly(lactic acid) (PLA). PLA has remarkable performances which are utilized in various applications (*e.g.* transparency, high tensile strength, and biocompatibility). However, PLA has relatively short shelf life,^{12,13} at the same time, the disposal items for general purposes, produced from PLA, have not been satisfied since the sales revenue level is below the break-even point. Considering the mulch film, it is a challenged and promising field for PLA film; however, there were few reports. For instance, Finkenstadt and Tisserat (2010) proposed PLA/Osage orange wood fiber composite which exhibited the fully biodegradability, growth promotion and controlled release of organic compounds into the soil, including cost effectiveness.¹⁴

The fact that the brittleness of PLA film is another considered point for developing as the practical mulch film. This is caused by high glass transition temperature of PLA ($T_g \sim 60^\circ\text{C}$) and slow crystallization rate with low degree of crystallinity ($X_c \sim 3\%$). Many nucleating agents (*e.g.* talc, montmorillonite, and starch) and plasticizers (*e.g.* polyethylene glycol and glycerol) have been revealed in order to improve toughness for PLA film.¹⁵⁻¹⁹ Thermoplastic starch (TPS) is an attractive additive for either conventional or biodegradable thermoplastic polymers due to natural abundance, fully biodegradability and high viscoelasticity.²⁰⁻²⁶ Basically, the melting temperature of starch is nearby its degradation temperature so it is difficult to be processed by simply melt blending. When the starch was

gelatinized with water or glycerol to form TPS, it is a breakthrough to extend processability by decreasing of melting temperature of starch.^{27,28}

In the case of PLA/TPS blend, it was also widely investigated in order to balance cost effectiveness with remained good performances (*e.g.* flexibility, fully biodegradation and relatively short shelf life).^{25,29,30} In addition, most studies used a reactive compatibilizer (*i.e.* maleic anhydride) to enhance miscibility between PLA and TPS for improved mechanical properties.²⁹⁻³² Lately, our group succeeded in the reactive PLA/starch blend via the simple coupling reaction by using chloropropyl trimethoxysilane (CPMS). The PLA blended with CPMS modified-starch (PLA/CP-starch) allowed the significant improved miscibility and also increased degree of PLA crystallinity.³³

It comes to our viewpoint that the PLA/CPMS-modified-TPS (PLA/mTPS) film is challenged for developing as the practical mulch film. How the combined properties of PLA and mTPS in the blend system are, and consequently, whether PLA/mTPS film is effectively utilized as biodegradable mulch film, are still questioned.

In this work, the PLA/mTPS films were systematically produced and carefully studied for further potential use as mulch film. The processability, miscibility improvement, and crystallization behavior of PLA/mTPS film with the consequences of oxygen permeability, tensile properties as well as degradation ability were also illustrated.

5.3 Materials and Experimental

5.3.1 Materials

PLA 2003D with a density of 1.24 g/cm³ and a melt flow rate of 6 g/10 min at 210 °C and 2.16 kg load was from NatureWorks LLC, USA. Cassava starch and glycerol were purchased from ETC International Trading Co., Ltd., and Siam Absolute Chemicals Co., Ltd., Thailand, respectively. 3-Chloropropyl trimethoxysilane (CPMS) with 97% purity was bought from Sigma-Aldrich, Germany.

5.3.2 Sample Preparations

5.3.2.1 *TPS and mTPS Preparation*

CPMS (0.05 mol, 9.9 mL) was hydrolyzed with deionized water until its turbidity was vanished at 50 °C before premixing with dried cassava starch (1 mol, 162.0 g) and drying at 70 °C in a hot air oven for 6 h as reported in our previous study.³³ After that, the CP-starch was mixed with glycerol at a 70/30 weight ratio before gelatinizing by a Labtech Engineering LTE 20-40 counter-rotating twin screw extruder. The temperature and screw speed were in the range of 100-150 °C and 40-50 rpm, respectively. Similarly, pure cassava starch was mixed with glycerol to prepare TPS.

5.3.2.2 *PLA/TPS and PLA/mTPS Films*

The mTPS obtained was blended with the PLA resin with the weight ratios (PLA/mTPS) of 90/10, 80/20, 70/30, 60/40, and 50/50 w/w by the counter-rotating twin screw extruder. The temperature and screw speed were in the range of 150-165°C and 25-40 rpm, respectively. The blend was blown to produce the PLA/mTPS film with ~0.20 mm thickness by using a Labtech Engineering LE 20-30 single-screw extruder equipped with a Labtech Engineering LF-400 blown film unit. The other film, *i.e.*, PLA/TPS, was prepared in the similar procedure.

5.3.3 Characterization

5.3.3.1 *Contact Angle Measurement*

The contact angle of water on TPS and mTPS was measured by a KRÜSS DSA 10 drop shape analysis system.

5.3.3.2 *Morphological and Topological Observations*

The cross-section surfaces of PLA/TPS and PLA/mTPS films coated with a thin layer of platinum were investigated by a Hitachi TM3000 scanning electron microscope (SEM) at accelerating voltages of 5 kV in SE mode. The topology of each film surface was also observed by a Park Systems XE-100 atomic force microscope (AFM) under a non-contact mode with a 910M-ACTA cantilever. The AFM measurement was operated at a scan speed of 0.4 Hz with a scan area of 5 x 5 μm².

5.3.3.3 Thermal Analysis

Thermal analysis was evaluated by a Netzsch 200 F3 Maia differential scanning calorimetry (DSC), the sample (10 mg) was packed in an aluminium pan and heated from -20 °C to 200 °C with a heating rate of 5°C/min under nitrogen flow (50 mL/min). The degree of crystallinity (X_c) of PLA was calculated by using Eq. (1):

$$X_c (\%) = \frac{\Delta H_{m, PLA} \times 100}{f \times \Delta H_m^0} \quad (\text{Eq. 1})$$

where $\Delta H_{m, PLA}$ is the observed enthalpy change of PLA fusion, f is the PLA weight fraction in blend, and ΔH_m^0 is 93.0 J/g regarding to the melting enthalpy of 100% crystalline PLA.³⁴

5.3.3.4 Oxygen Permeability Measurement

Oxygen permeability was evaluated by an Ox-Tran 2/21 MOCON oxygen analyzer with oxygen flow rate of 20 cm³/min at 23 °C at 0% RH (relative humidity), according to ASTM D3985-81.

5.3.3.5 Testing of Mechanical Properties

The film samples were cut into 2.5×15.0 cm². The tensile properties of the films were measured at 25°C with a tensile load of 5 kN and a cross-head speed of 500 mm/min according to ASTM D882 by using an Instron 4206 universal testing machine. The deformation occurred along machine direction and the average reported values for mechanical test were based on 10 specimens.

5.3.3.6 QUV Accelerated Weathering Simulation and Determination of a Remained Molecular Weight

The selected samples were cut into 2.5 × 15.0 cm² and air-dried at 80 ± 3 °C for 20 h before testing. The simulated weathering was carried out according to ASTM G154 cycle 5 by an Accelerated Weathering QUV/Spray tester under fluorescent lamps UVB-313. The irradiance of the peak emission was 0.62 W/m² at wavelength of 310 nm.

Furthermore, the number average molecular weight (\overline{M}_n), the weight average molecular weight (\overline{M}_w), and polydispersity index (PDI) of the samples after simulated weathering test were determined by a Shimadzu Class-VP gel permeation chromatography (GPC). Those samples were eluted in HPLC-grade

chloroform through a Polymer Lab PL gel 5 μm MIXED-D column with an isocratic mobile phase at a flow rate of 1 mL/min and at 40 °C. The samples were filtered with as 0.45 μm before injected into a 20 μL injection loop.

5.4 Results and Discussion

5.4.1 Hydrophobicity Improvement of mTPS

Basically, the difference between the hydrophobic PLA and the hydrophilic starch causes the phase separation in PLA/starch blends; therefore, the modification of starch for hydrophobicity improvement is a promising approach to enhance miscibility. A water contact angle measurement (Figure 5.1) was used to determine the improved hydrophobic surface of starch and TPS after coupling with CPMS. Figure 5.1a shows the water contact angle of PLA as high as 70°, indicating the relatively high hydrophobicity whereas 0° water contact angle exhibits for starch (Figure 5.1b). After starch was gelatinized to form TPS for processability, it shows the water contact angle of 9° (Figure 5.1d), suggesting the slightly hydrophobic surface improvement. It implies that the glycerol addition might interrupt the inter- and intramolecular hydrogen bonds in starch molecules as also investigated by Jiugao *et al* (2005).³⁵ This should be noted that TPS formation can provide not only melt processability but also the faintly increased hydrophobicity of starch.

In case of mTPS, Figure 5.1e presents the water contact angle of 45°, higher than that of TPS. It reflects the promoted hydrophobicity by coupling of aliphatic chains of CPMS on pyranose rings, as reported in our previous work.³³ This significantly enhanced hydrophobicity of mTPS possibly assists miscibility with PLA. However, mTPS shows the lower water contact angle than that of CP-starch (60° water contact angle). This could be caused by the hydroxyl groups of glycerol interaction with water.

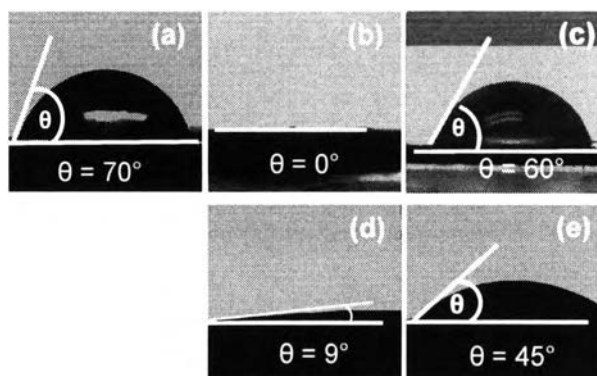


Figure 5.1 Water contact angles of (a) PLA film, (b) starch, (c) CP-starch, (d) TPS, and (e) mTPS.

It comes to the question that how the different hydrophobicity improvement of TPS and mTPS effects on the morphology of PLA/TPS and PLA/mTPS blends as well as the other performances of those blown films such as surface topology, PLA crystallization behavior and mechanical properties.

5.4.2 Morphological and Topological Observations

5.4.2.1 *Morphology of PLA/TPS and PLA/mTPS Blends*

The TPS and mTPS obtained were blended with commercial PLA resin at various weight ratios (*i.e.* PLA/TPS or mTPS: 90/10, 80/20, 70/30, 60/40, and 50/50 w/w) before they were blown to be PLA/TPS and PLA/mTPS films. In order to clarify the miscibility improvement, the SEM technique was used for studying the cross-section morphology of PLA/TPS or mTPS blends.

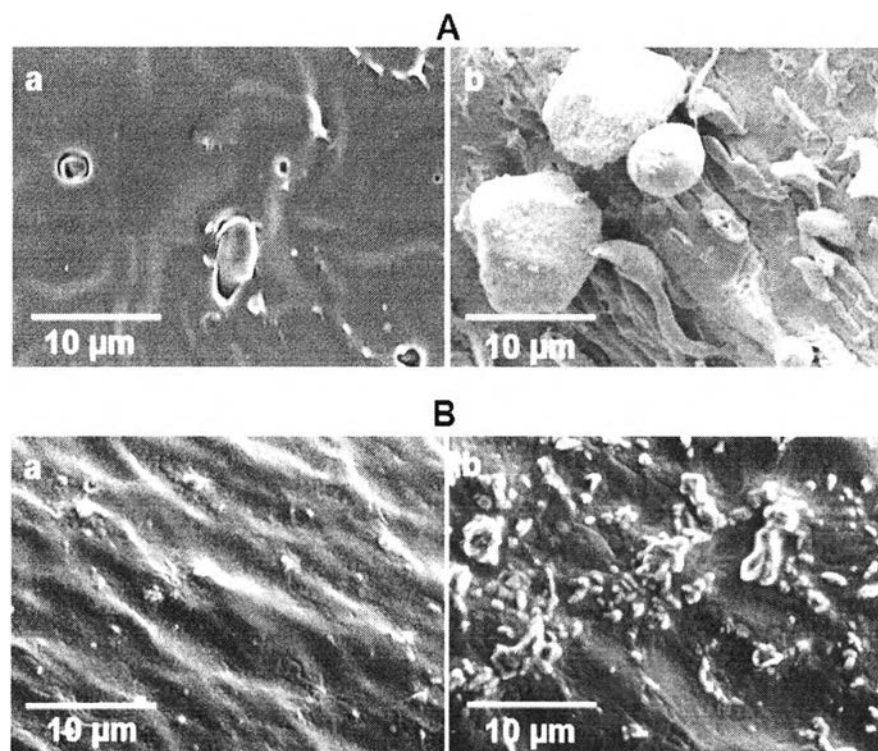


Figure 5.2 SEM micrographs of cross-section surfaces of (A) PLA/TPS and (B) PLA/mTPS blends at weight ratios of (a) 90/10 and (b) 50/50 (w/w).

The partial phase separation is observed in PLA/TPS 90/10 (Figure 5.2A, a) whereas the relatively homogeneous blend is found in PLA/mTPS 90/10 (Figure 5.2B, a). When the TPS content was increased to 50 %wt, the agglomeration of TPS phase in PLA matrix occurred obviously (Figure 5.2A, b). Contrary to PLA/mTPS 50/50, the finer dispersion of mTPS phase in PLA matrix than that of PLA/TPS, was obtained as seen in Figure 5.2B. b. This reflects the successful miscibility improvement by starch chemically modified with silane coupling agent. Additionally, the enhanced hydrophobicity of mTPS also assists to promote the good dispersion in the PLA/mTPS blend.

5.4.2.2 Topology of PLA/TPS and PLA/mTPS Films

Furthermore, after the PLA/TPS and PLA/mTPS blends were blown, the films obtained were carefully investigated the miscibility in nanoscale by using AFM microscope. The surface topology images with roughness average (R_a),

and maximum height of the profile (R_T) are shown in Figure 5.3. The R_a is the arithmetic mean of the absolute values of the height of the surface profile whereas the R_T is defined as the vertical distance between the deepest valley and the highest peak, in other words, the low R_a and R_T values imply the highly homogeneous and smooth surface, reflecting the good miscibility in the blend.

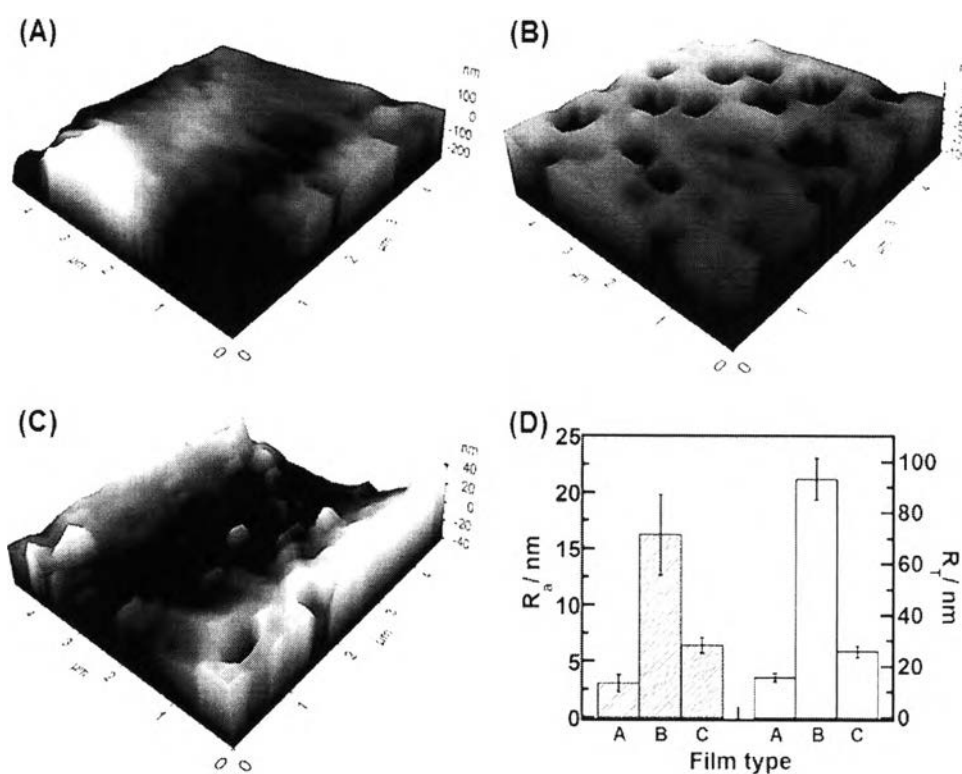


Figure 5.3 Surface topology images of (A) PLA, (B) PLA/TPS 50/50, and (C) PLA/mTPS 50/50 films as observed by AFM and (D) determined R_a (stripe) and R_T (blank) of each film.

Figure 5.3A shows the surface topology of the PLA blown film which is highly smooth with R_a 3 nm and R_T 15 nm. In the case of PLA/TPS 50/50 (Figure 5.3B), a lot of voids are found on the surface with significantly increased R_a and R_T as high as 16 nm and 95 nm, respectively. These indicate the extremely different height from peak to baseline, reflecting a rough surface which is due to the immiscibility between PLA and TPS phases. Oppositely, the relative smoothness of the PLA/mTPS 50/50 film surface was observed clearly from its

surface topology with decreased R_a (6 nm) and R_T (28 nm). This result firmly insists the successful miscibility improvement by PLA chemically bound with mTPS.

5.4.3 Physical Properties of PLA/TPS and PLA/mTPS Films

5.4.3.1 *Crystallization Behavior*

In order to illustrate the influences of TPS and/or mTPS blending on PLA crystallization change which directly manifests the mechanical and barrier properties, the thermal analysis was carried out by using DSC technique with the first heating scan. Figure 5.4 shows the glass transition temperature (T_g) and degree of crystallinity (X_c) of PLA as a function of TPS and/or mTPS content in the blended films.

It is well known that the T_g of PLA exhibits, higher than the room temperature, at ~ 60 °C and the PLA crystallization rate is very slow with X_c 3-5%, resulting in brittleness. In the case of the PLA/TPS films, the T_g is gradually decreased to 49 °C when TPS content is increased from 10 %wt to 30 %wt. The T_g is remained at ~ 50 °C although the TPS content is higher than 40 %wt (Figure 5.4A). Meanwhile, the X_c of PLA is drastically increased from 5% to 30% by addition of TPS 10 %wt (Figure 5.4B). With increasing amount of TPS to 50 %wt, the X_c of PLA gradually increased to 42%. This points out that dual functions of TPS (*i.e.* starch as nucleating agent and glycerol as plasticizer) promote the PLA chains movement in amorphous region, and consequently, the ordered chain packing for crystallization, as evidenced from decreased T_g and enlarged X_c .

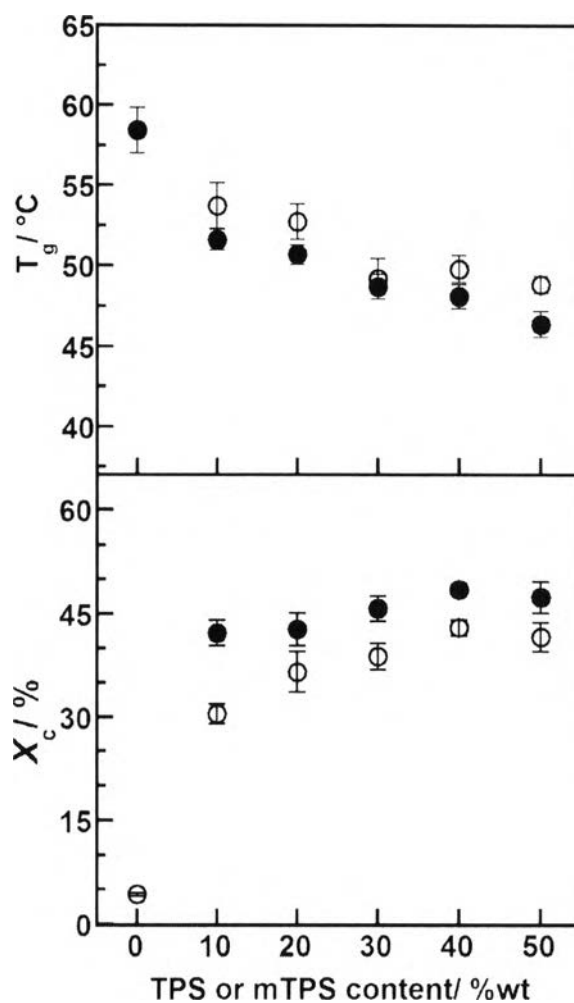


Figure 5.4 T_g and X_c values of PLA/TPS (open) and PLA/mTPS (closed) films.

In the similar way, for PLA/mTPS films, the T_g of PLA is also decreased to 52 °C by adding 10 %wt mTPS, and continuously to 47 °C by increasing of mTPS content. Remarkably, these reduced T_g s in the PLA/mTPS films are more significant than those of the PLA/TPS films.

This might reflect to the improved miscibility between PLA and mTPS which assists the PLA chain movement much easier than that of the PLA/TPS case. Additionally, the X_c of PLA is enhanced for almost 10 times by adding 10 %wt mTPS. The X_c obtained from the PLA/mTPS film was saturated at the level as high as 45-50% although the mTPS content was increased.

5.4.3.2 Oxygen Permeability

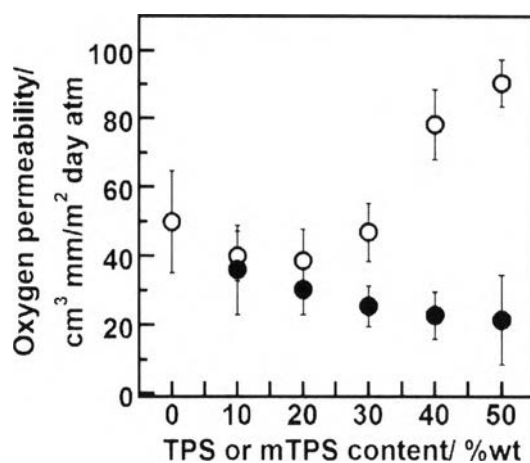


Figure 5.5 Oxygen permeability of PLA/TPS (open) and PLA/mTPS (closed) films.

Oxygen permeability is an important parameter for mulch film which plays an important role on microbial activity in soil.³⁶ The appropriate oxygen permeability value for each mulch film depends on plant species. Normally, this parameter can be controlled directly by crystalline region of polymer matrix which functions as barrier for gas permission. The higher X_c in the film is created, the lower oxygen permeability is obtained, as also revealed by Guinault *et al* (2012).³⁷ Pure PLA film shows the oxygen permeability of ~ 50 cm³ mm/m² day atm which is relatively low as compared to conventional plastics such as low-density polyethylene film (>100 cm³ mm/m² day atm), reported by Massey (2003).³⁸

After PLA blending with TPS, the oxygen permeabilities of the PLA/TPS 90/10 and 80/20 films are vaguely reduced to 40 cm³ mm/m² day atm before the value is gradually elevated to 50, 80, and 95 cm³ mm/m² day atm for 30, 40, and 50 %wt TPS contents (Figure 5.5). This increment of oxygen permeability possibly comes from the immiscibility between TPS and PLA phases. Although the X_c of the film is as high as $\sim 45\%$, there were some voids around TPS phase in PLA matrix, as presented in SEM images (Figure 5.2A), which allows the oxygen gas to permeate easily.

In contrast, the oxygen permeability of the PLA/mTPS film is diminished continuously from 40 to 20 cm³ mm/m² day atm, correlating to the X_c increment by adding mTPS. This result might be from a combination of (i) high X_c of PLA induced by dually functional mTPS and (ii) the continuous phase of PLA/mTPS blend. It should be noted that not only the X_c but also the miscibility between PLA/mTPS phases strongly influence on the oxygen barrier property.

5.4.3.3 Mechanical Properties

In general, PLA is classified as a rigid and brittle polymer with relatively high Young's modulus (E 2.3 GPa), high tensile strength (σ 45 MPa), and very low elongation at break (ϵ 3%). These mechanical properties limit usability of PLA in various applications. Blending PLA with any compounds is needed to extend its utilization.

After blending with 10 %wt TPS, the E is significantly dropped to 1 GPa. However, it is increased to 2.5 GPa by increasing TPS content (Figure 5.6A). Whereas the E of PLA/mTPS film gradually decreased from 1.8 GPa to 1 GPa when mTPS content was increased from 10 %wt to 50 %wt, respectively. It implies that some voids in the PLA/TPS film obstruct the stress distribution when the deformation during tensile test was occurred. Thus, high force was required to stretch the PLA/TPS film. But, in the case of PLA/mTPS, the miscibility improvement between mTPS and PLA matrix assists to distribute the tensile stress occurred. The deformation was easily performed.

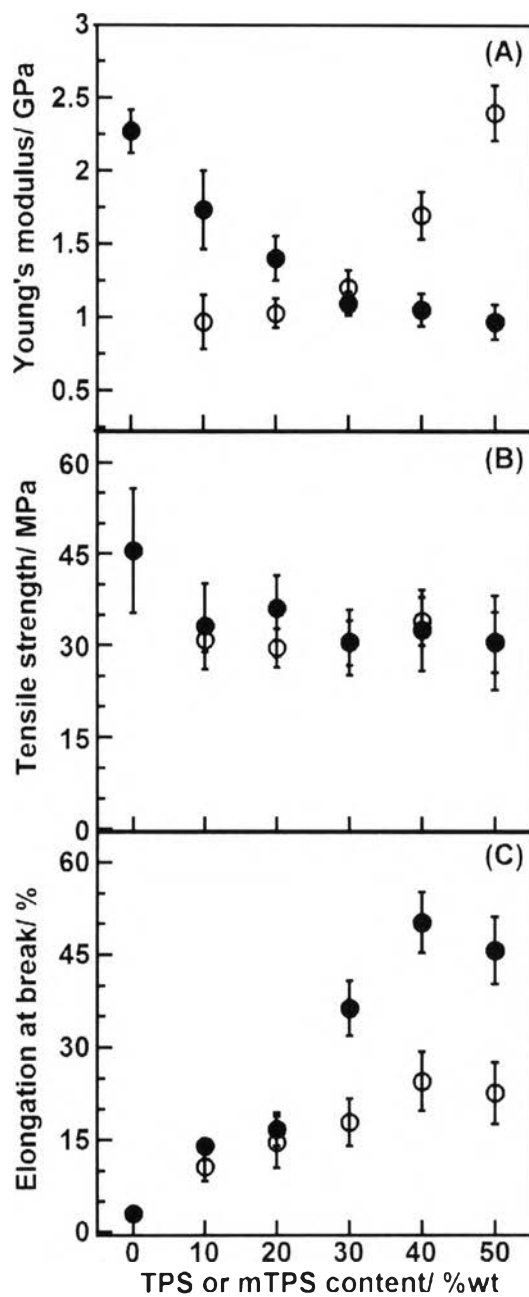


Figure 5.6 (A) Young's modulus, (B) tensile strength, and (C) elongation at break of PLA/TPS (open) and PLA/mTPS (closed) films.

At the same time, the trends of σ for both PLA/TPS and PLA/mTPS films are quite similar (Figure 5.6B). The slightly reduced σ values by addition of TPS and/or mTPS are in the range of 30-35 MPa, independent on the content. This decreased σ might be from the addition of flexible polymer (*i.e.* TPS

and/or mTPS) which reduced the rigidity of the PLA films. As anticipated, the ϵ of the PLA/TPS and PLA/mTPS films are remarkably enhanced as shown in Figure 5.6C. The highest ϵ value is presented by PLA/mTPS 60/40 (ϵ 52%) while PLA/TPS 60/40 shows the ϵ of 25%. The successfully improved flexibility to PLA is related to not only the decreased T_g by consisting of glycerol as plasticizer in the film but also the homogenous blending of PLA/mTPS. It can be concluded that the brittle PLA film becomes flexible with low oxygen permeability when PLA was blended with mTPS.

5.4.4 Degradation Investigation through Weathering Simulation

Considering the overall investigated properties, based on increased crystallinity, flexibility improvement, and high content of TPS or mTPS in the blend, the films with 60/40 blending weight ratio were selected to further preliminary trace on degradation by weathering simulation at varied periods of study time.

After passing simulated weather which was equivalent to 1 month of real-time radiation exposure, the PLA film shows a little shrinkage with remained high transparency as seen in Figure 5.7A. When the real-time radiation exposure was increased to be for 2 months, more shrinkage without cracking on PLA film was observed before it became opaque and the cracking was initiated at the end of the 4th month of real-time radiation exposure. This indicates the relatively high tolerance of PLA film to be degraded under UV irradiation.

In the case of the PLA/TPS 60/40 film (Figure 5.7B), the shrinkage occurred obviously since the real-time radiation exposure was 1 month. This film was more opaque and brownish than an original one (0 month, before QUV accelerated weathering testing). It completely degraded after it was exposed for 2 months real-time radiation. Different from the PLA/TPS film, some parts of PLA/mTPS 60/40 film (Figure 5.7C) had partially preserved itself in the film-form although the simulated weather for either 2- or 4-month real-time radiation was applied. This implies that the miscibility improvement by mTPS may assist the dimensional stability somehow. Additionally, the degradation of PLA could be accelerated by TPS or mTPS blending because TPS and mTPS are derived from

biopolymer which is sensitive to UV radiation, as reported by Dintcheva and Mantia (2007).³⁹

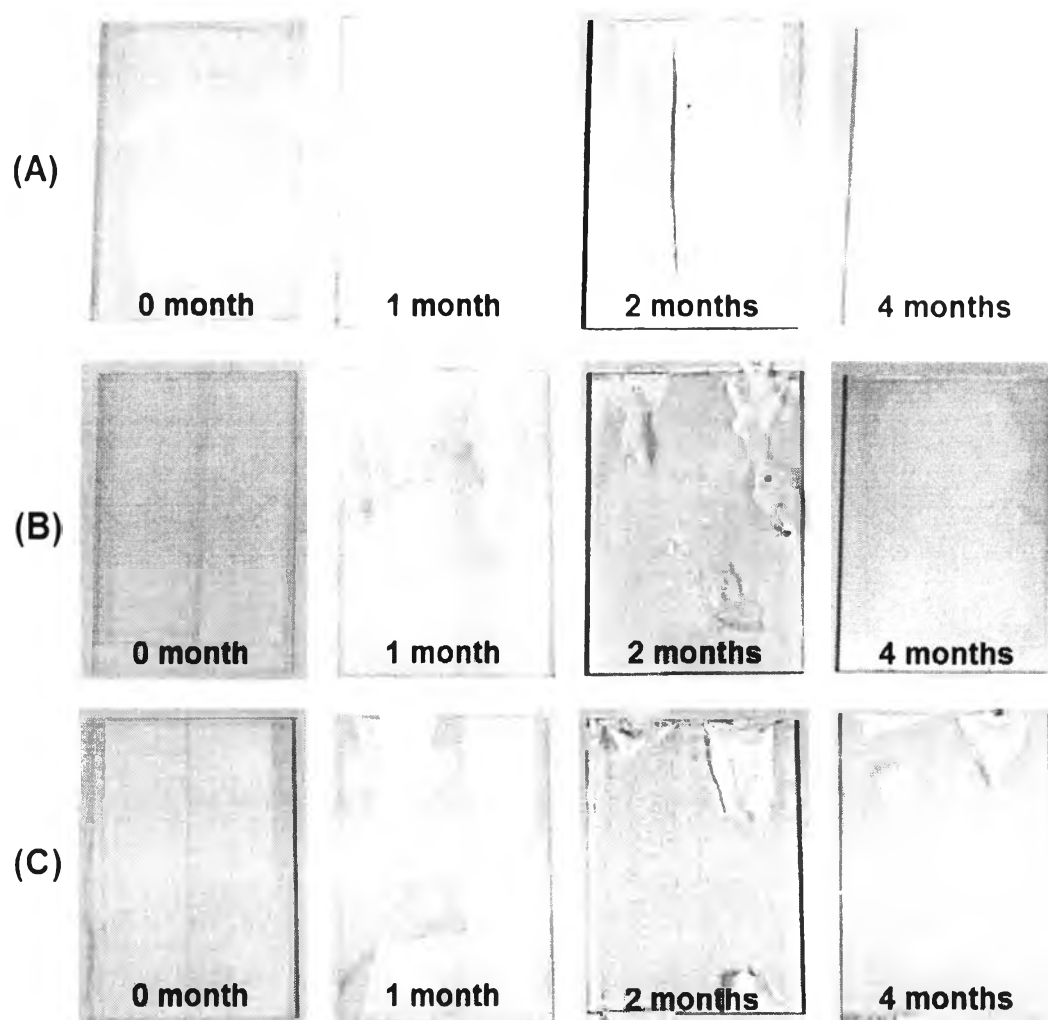


Figure 5.7 Appearance of (A) PLA, (B) PLA/TPS 60/40, and (C) PLA/mTPS 60/40 films after QUV accelerated weathering test at various time periods.

In order to make a concrete discussion, the quantitative analysis of PLA molecular weight by GPC technique was carried out for PLA, PLA/TPS, and PLA/mTPS films after simulated weather testing at varied periods of real-time radiation exposure (Table 5.1).

The \overline{M}_w and \overline{M}_n of PLA film gradually decrease (from 21×10^4 and 20×10^4 g/mol to 12×10^4 and 6×10^4 g/mol, respectively) with slightly increased PDI (from 1.1 to 2.2) when the real-time radiation exposure was increased.

Table 5.1 \overline{M}_w and \overline{M}_n with PDI of PLA, PLA/TPS 60/40, and PLA/mTPS 60/40 films after QUV accelerated weathering test at various periods of time.

Film type	Time periods (months)	$\overline{M}_w \times 10^4$ (g/mol)	$\overline{M}_n \times 10^4$ (g/mol)	PDI
PLA	0	21.1 ± 1.1	20.0 ± 1.0	1.1 ± 0.1
	1	19.9 ± 0.9	14.5 ± 1.2	1.4 ± 0.2
	2	17.6 ± 1.1	12.2 ± 1.5	1.5 ± 0.3
	3	15.8 ± 1.0	8.4 ± 1.1	1.9 ± 0.1
	4	12.2 ± 1.5	5.7 ± 0.4	2.2 ± 0.3
PLA/TPS 60/40	0	18.7 ± 1.8	11.7 ± 1.5	1.6 ± 0.2
	1	4.9 ± 0.7	1.6 ± 0.3	3.2 ± 0.2
	2	2.5 ± 0.3	1.0 ± 0.1	2.7 ± 0.1
	3	2.0 ± 0.1	0.7 ± 0.1	2.6 ± 0.4
	4	1.2 ± 0.2	0.4 ± 0.1	2.9 ± 0.2
PLA/mTPS 60/40	0	16.7 ± 1.3	12.4 ± 0.6	1.3 ± 0.1
	1	5.2 ± 0.7	1.6 ± 0.3	3.4 ± 0.3
	2	3.6 ± 0.4	1.6 ± 0.2	2.4 ± 0.2
	3	2.6 ± 0.5	1.0 ± 0.1	2.7 ± 0.2
	4	1.7 ± 0.2	0.7 ± 0.2	2.4 ± 0.4

Similarly, the drastic declined \overline{M}_w and \overline{M}_n of PLA/TPS film are obtained with considerably broad PDI when the real-time radiation exposure was for 4 months (from \overline{M}_w 18.7×10^4 g/mol to 1.2×10^4 g/mol, \overline{M}_n 11.7×10^4 g/mol to 0.4×10^4 g/mol, and PDI 1.6 to 2.9, for 0 and 4 months, respectively). Meanwhile, the \overline{M}_w and \overline{M}_n of PLA/mTPS film exposed for 4 months real-time are decreased to be 1.7×10^4 g/mol and 0.7×10^4 g/mol, respectively, with relatively broad PDI (2.4).

This result suggests the relatively slow degradation rate of PLA film as indicated by the higher remained \overline{M}_w and \overline{M}_n of PLA with lower PDI than those of PLA/TPS and PLA/mTPS films. It should be noted that the degradation rate of PLA was accelerated by blending with TPS and/or mTPS due to highly-moisture, temperature, and UV sensitive compound, *i.e.*, starch and glycerol consisting in either TPS or mTPS.

Comparing the cases of PLA/TPS and PLA/mTPS films, the remained \overline{M}_w and \overline{M}_n after simulated degradation of PLA/mTPS films are clearly higher than those of PLA/TPS films. This confirms the prolonged stability of PLA/mTPS film which plays a key role on the further trial of appropriate life cycle of mulch film for plant growth.

5.5 Conclusions

The present work proposed the PLA/mTPS film as a potential biodegradable mulch film. The chemically modified mTPS can successfully enhance miscibility with well dispersion in PLA matrix, and consequently, promote the PLA chain mobility as observed from decreased T_g with high $X_c \sim 50\%$. The enhanced PLA crystallinity with homogeneous blend acts as effective barrier for oxygen with 50% reduction as compared to the pure PLA film. The film flexibility was also improved significantly with 10-fold increased ϵ (52%) by mTPS 40 %wt and maintained relatively high σ (30 MPa) as compared to the PLA film. The PLA/mTPS 60/40 film also performed the acceleration of slow PLA degradation and prolonged the durability after simulated weathering exposure for 4 months of real-time as evidenced from both qualitative and quantitative analyses.

5.6 Acknowledgements

The authors would like to thank The Thailand Research Fund (the Royal Golden Jubilee Ph.D scholarship program PHD/0188/2550) and The National Research Council of Thailand research grant (2556-66 for the 2013-2014 academic

years) for financial supports. In addition, we are thankful to Labtech Engineering Co., Ltd. for the blending and blown film facilities. Center for Petroleum, Petrochemical, and Advanced Materials, Chulalongkorn University and Wandee Plastic Agencies Co., Ltd. are also acknowledged.

5.7 References

- (1) Espí, E.; Salmerón, A.; Fontecha, A.; García, Y.; Real, A. I. *Journal of Plastic Film and Sheeting* **2006**, *22*, 85.
- (2) Briassoulis, D. *Polymer Degradation and Stability* **2007**, *92*, 1115.
- (3) Briassoulis, D.; Aristopoulou, A.; Bonora, M.; Verloot, I. *Biosystems Engineering* **2004**, *88*, 131.
- (4) Abrusci, C.; Pablos, J. L.; Marín, I.; Espí, E.; Corrales, T.; Catalina, F. *International Biodeterioration & Biodegradation* **2013**, *83*, 25.
- (5) Koutny, M.; Lemaire, J.; Delort, A.-M. *Chemosphere* **2006**, *64*, 1243.
- (6) Hagström, B.; Malmros, P.; Google Patents: 2008.
- (7) Kyrikou, I.; Briassoulis, D. *Journal of Polymers and the Environment* **2007**, *15*, 125.
- (8) Kijchavengkul, T.; Auras, R.; Rubino, M.; Ngouajio, M.; Fernandez, R. T. *Chemosphere* **2008**, *71*, 942.
- (9) Bilck, A. P.; Grossmann, M. V. E.; Yamashita, F. *Polymer Testing* **2010**, *29*, 471.
- (10) Stloukal, P.; Verney, V.; Commereuc, S.; Rychly, J.; Matisova-Rychlá, L.; Pis, V.; Koutny, M. *Chemosphere* **2012**, *88*, 1214.
- (11) Scarascia-Mugnozza, G.; Schettini, E.; Vox, G.; Malinconico, M.; Immirzi, B.; Pagliara, S. *Polymer Degradation and Stability* **2006**, *91*, 2801.
- (12) Tawakkal, I. S. M. A.; Cran, M. J.; Miltz, J.; Bigger, S. W. *Journal of Food Science* **2014**, *79*, R1477.
- (13) Peelman, N.; Ragaert, P.; Vandemoortele, A.; Verguldt, E.; De Meulenaer, B.; Devlieghere, F. *Innovative Food Science & Emerging Technologies*.
- (14) Finkenstadt, V. L.; Tisserat, B. *Industrial Crops and Products* **2010**, *31*, 316.
- (15) Auras, R.; Harte, B.; Selke, S. *Macromolecular bioscience* **2004**, *4*, 835.

- (16) Garlotta, D. *Journal of Polymers and the Environment* **2002**, *9*, 63.
- (17) Labrecque, L. V.; Kumar, R. A.; Davé, V.; Gross, R. A.; McCarthy, S. P. *Journal of Applied Polymer Science* **1997**, *66*, 1507.
- (18) Kang, K.; Lee, S.; Lee, T.; Narayan, R.; Shin, B. *Korean J. Chem. Eng.* **2008**, *25*, 599.
- (19) Zhang, R.; Wang, Y.; Wang, K.; Zheng, G.; Li, Q.; Shen, C. *Polymer Bulletin* **2012**, *70*, 195.
- (20) Shujun, W.; Jiugao, Y.; Jinglin, Y. *Polymer Degradation and Stability* **2005**, *87*, 395.
- (21) Rodriguez-Gonzalez, F. J.; Ramsay, B. A.; Favis, B. D. *Polymer* **2003**, *44*, 1517.
- (22) Taguet, A.; Huneault, M. A.; Favis, B. D. *Polymer* **2009**, *50*, 5733.
- (23) Sarazin, P.; Li, G.; Orts, W. J.; Favis, B. D. *Polymer* **2008**, *49*, 599.
- (24) Ning, W.; Jiugao, Y.; Xiaofei, M.; Ying, W. *Carbohydrate Polymers* **2007**, *67*, 446.
- (25) Müller, C. M. O.; Pires, A. T. N.; Yamashita, F. *Journal of the Brazilian Chemical Society* **2012**, *23*, 426.
- (26) Wang, N.; Yu, J.; Chang, P. R.; Ma, X. *Carbohydrate Polymers* **2008**, *71*, 109.
- (27) Shogren, R. L. *Carbohydrate Polymers* **1992**, *19*, 83.
- (28) Jang, J. K.; Pyun, Y. R. *Starch - Stärke* **1996**, *48*, 48.
- (29) Ren, J.; Fu, H.; Ren, T.; Yuan, W. *Carbohydrate Polymers* **2009**, *77*, 576.
- (30) Zhang, J.-F.; Sun, X. *Macromolecular bioscience* **2004**, *4*, 1053.
- (31) Li, H.; Huneault, M. A. *International Polymer Processing* **2008**, *23*, 412.
- (32) Huneault, M. A.; Li, H. *Polymer* **2007**, *48*, 270.
- (33) Jariyasakoolroj, P.; Chirachanchai, S. *Carbohydrate Polymers* **2014**, *106*, 255.
- (34) Fischer, E. W.; Sterzel, H.; Wegner, G. *Kolloid-Z.u.Z.Polymere* **1973**, *251*, 980.
- (35) Jiugao, Y.; Ning, W.; Xiaofei, M. *Starch - Stärke* **2005**, *57*, 494.
- (36) Acharya, C. L.; Hati, K. M.; Bandyopadhyay, K. K. In *Encyclopedia of Soils in the Environment*; Hillel, D., Ed.; Elsevier: Oxford, 2005, p 521.

- (37) Guinault, A.; Sollogoub, C.; Ducruet, V.; Domenek, S. *European Polymer Journal* **2012**, *48*, 779.
- (38) Massey, L. K. In *Permeability Properties of Plastics and Elastomers (Second Edition)*; Massey, L. K., Ed.; William Andrew Publishing: Norwich, NY, 2003, p 209.
- (39) Dintcheva, N. T.; La Mantia, F. P. *Polymer Degradation and Stability* **2007**, *92*, 630.